OXFORD

RESEARCH ARTICLE

Depressive-Like Behavior Is Paired to Monoaminergic Alteration in a Murine Model of Alzheimer's Disease

Adele Romano, PhD[*]; Lorenzo Pace, MSc[*]; Bianca Tempesta, MSc;
Angelo Michele Lavecchia, MSc; Teresa Macheda, PhD; Gaurav Bedse, PhD;
Antonio Petrella, DVM; Carlo Cifani, PhD; Gaetano Serviddio, MD;
Gianluigi Vendemiale, MD; Silvana Gaetani, PhD; Tommaso Cassano, PhD

[*] These authors contributed equally as first authors.
Department of Physiology and Pharmacology, Sapienza University of Rome, Italy (Drs Romano, Tempesta, Lavecchia, Bedse, and Gaetani); Department of Clinical and Experimental Medicine, University of Foggia, Italy (Drs Pace, Macheda, and Cassano); Puglia and Basilicata Experimental Zooprophylactic Institute, Foggia, Italy (Dr Petrella); School of Pharmacy, Pharmacology Unit, University of Camerino, Italy (Dr Cifani); Department of Medical and Surgical Sciences, University of Foggia, Italy (Drs Serviddio and Vendemiale).

Correspondence: Tommaso Cassano, PhD, Department of Clinical and Experimental Medicine, University of Foggia, Viale Luigi Pinto 1, Foggia 71100, Italy (tommaso.cassano@unifg.it).

Abstract

Background: Neuropsychiatric signs are critical in primary caregiving of Alzheimer patients and have not yet been fully investigated in murine models.
Methods: 18-month-old 3×Tg-AD male mice and their wild-type male littermates (non-Tg) were used. The open field test and the elevated plus maze test were used to evaluate anxiety-like behaviors, whereas the Porsolt forced swim test, the tail suspension test, and the sucrose preference test for antidepressant/depression-coping behaviors. Neurochemical study was conducted by microdialysis in freely-moving mice, analyzing the basal and K$^+$-stimulated monoamine output in the frontal cortex and ventral hippocampus. Moreover by immunohistochemistry, we analysed the expression of Tyrosin hydroxylase and Tryptophan hydroxylase, which play a key role in the synthesis of monoamines.
Results: Aged 3×Tg-AD mice exhibited a higher duration of immobility in the forced swim and tail suspension tests (predictors of depression-like behavior) which was not attenuated by a noradrenaline reuptake inhibitor, desipramine. In the sucrose preference test, 3×Tg-AD mice showed a significantly lower sucrose preference compared to the non-Tg group, without any difference in total fluid intake. In contrast, the motor functions and anxiety-related emotional responses of 3×Tg-AD mice were normal, as detected by the open-field and elevated plus-maze tests. To strengthen these results, we then evaluated the monoaminergic neurotransmissions by in vivo microdialysis and immunohistochemistry. In particular, with the exception of the basal hippocampal dopamine levels, 3×Tg-AD mice exhibited a lower basal extracellular output of amines in the frontal cortex and ventral hippocampus and also a decreased extracellular response to K$^+$ stimulation. Such alterations occur with obvious local amyloid-β and tau pathologies and without gross alterations in the expression of Tyrosin and Tryptophan hydroxylase.
Conclusions: These results suggest that 3×Tg-AD mice exhibit changes in depression-related behavior involving aminergic neurotrasmitters and provide an animal model for investigating AD with depression.

Keywords: anxiety, depression, frontal cortex, hippocampus, monoaminergic neurotransmission, triple transgenic model of AD

Introduction

Alzheimer's disease (AD) is characterized by progressive impairment of memory accompanied by neuropsychiatric disturbances (Assal and Cummings, 2002). Several studies have shown that depression is a risk factor for AD and that patients with mild cognitive impairment and depression have more than twice the risk of developing Alzheimer-type dementia than patients without depression (Steffens et al., 1997; Modrego and Ferrández, 2004). Although many pharmacological tools are currently available, different clinical studies suggest that the use of antidepressants as a class of medications for the treatment of depression in AD patients appears quite weak (Pomara and Sidtis, 2007; Sepehry et al., 2012). In this regard, many factors might account for the lack of a clear benefit of antidepressants in the comorbid depression (e.g. methods of assessment, diagnostic criteria, stages of the dementia; Sepehry et al., 2012). From the neurobiological perspective, we cannot exclude that amyloid-β (Aβ) and tau pathologies might alter the monoamine release into the synaptic cleave, interfering with the molecular mechanism of the antidepressants.

Hence, on the basis of the above considerations, it is possible to conclude that depression in AD is still not a well-understood phenomenon. Therefore, it might be urgent to further explore the monoaminergic alterations underlying the comorbid depression in AD, in order to explain the lack of the responsiveness to the therapy. In this regard, analysis of post-mortem brain tissue from patients with AD have revealed disturbances of the noradrenergic and serotonergic systems in the brain, whilst the results concerning the dopaminergic system are conflicting (Nyberg et al., 1985; Gottfries, 1990; Palmer and Dekosky, 1993). Most studies on the monoamine systems in AD have examined post-mortem material, which implies that the samples have been drawn from terminal cases and results were limited to correlational studies.

To better address the involvement of monoaminergic transmissions in the pathophysiology of depression in AD, animal models provide significant advantages that extend beyond mere correlation. In this regard, the triple transgenic model of AD (3×Tg-AD), which harbors three mutant human genes (APP$_{swe}$, PS1$_{M146V}$, and tau$_{P301L}$), has been one of the most thoroughly characterized (Oddo et al., 2003b). The 3×Tg-AD mice develop amyloid plaques and neurofibrillary pathology in a hierarchical manner in AD-relevant brain regions, and closely mimic the disease progression in humans (Oddo et al., 2003a, 2003b; Billings et al., 2005). More recently, we have demonstrated that 18-month-old 3×Tg-AD mice presented severe deficits in odor-based memory without gross changes in general odor-perceiving ability, and alterations in the glutamatergic transmission that co-exists with mitochondrial dysfunction (Cassano et al., 2011, 2012).

Moreover, 3×Tg-AD mice have been evaluated in tests of exploratory activity, including the open-field test (Giménez-LIort et al., 2007; Pietropaolo et al., 2008, 2009; Yao et al., 2009; Arsenault et al., 2011; Ojha et al., 2011) and elevated plus-maze (EPMT; Carroll et al., 2007). In the open-field test, there have been conflicting reports: hyperactivity in two studies (Giménez-LIort et al., 2007; Pietropaolo et al., 2008), hypoactivity in others (Nelson et al., 2007; Pietropaolo et al., 2009; Arsenault et al., 2011), or else no change (Ojha et al., 2011). In the EPMT, 3×Tg-AD mice displayed excessive anxiety relative to non-Tg mice in one study (Pietropaolo et al., 2009), but no change was reported in a second one (Pietropaolo et al., 2008). Therefore, in our study we sought to re-examine this question by evaluating exploratory activity in the open-field test and the EPMT and, mostly, to evaluate more comprehensively the depressive-like phenotype of 3×Tg-AD mice, which has not been fully investigated.

Furthermore, we investigated whether abnormalities in monoaminergic systems might co-exist with a depressive-like and/or anxiety-like behavior in our AD model. Neurochemical study was conducted by microdialysis in freely-moving mice, analyzing the basal and K⁺-stimulated monoamine output in the frontal cortex (FC) and ventral hippocampus (vHIPP), the two areas most affected by AD-pathologies and highly involved in the regulation of depressive-/anxiety-related behavior. Moreover by immunohistochemistry, we analysed the expression of Tyrosin hydroxylase (TH) and Tryptophan hydroxylase (TPH), which play a key role in the synthesis of neurotransmitters.

Materials and Methods

Subjects

18-month-old 3×Tg-AD male mice and their wild-type male littermates (non-Tg) were used. Colonies of 3×Tg-AD mice and non-Tg littermates were maintained under standard conditions (12:12 light–dark cycle; temperature at 22°C; 50–60% relative humidity; *ad libitum* access to food and water). The 3×Tg-AD mice background strain is C57BL6/129SvJ: hybrid and genotypes were confirmed according Oddo et al. (2003b).

All the experiments were performed in strict compliance with the Italian National Laws (DL 116/92) and the European Communities Council Directives (86/609/EEC). All efforts were made to minimize the number of animals used and their suffering.

Behavioral Assay

The open field test (OFT) and the EPMT were used to evaluate anxiety-like behaviors, whereas the Porsolt forced swim test (FST), the tail suspension test (TST), and the sucrose preference test (SPT) for antidepressant/depression-coping behaviors. A 3- to 4-day interim period was interlaced between tests. All tests were performed in a dimly lit environment and under minimal anxiogenic conditions. Behavior was videotaped with a camera and scored by an observer unaware of genotypes and treatments.

Anxiety-Related Tests

The OFT was performed as previously described (Cassano et al., 2011). Briefly, non-Tg and 3×Tg-AD mice were each placed at the center of the arena (28×28 cm white Plexiglas box with walls 15 cm high) and left to explore the whole field for 30 min of recording. The ethological measures analyzed included frequency and duration of rearing, thigmotaxis, time spent in self-grooming, and locomotor activity.

The EPMT was performed as previously described (Bambico et al., 2010). Briefly, the Plexiglas apparatus was raised 60 cm above ground and consisted of two opposite, open arms (30×5 cm) and two closed arms (30×5 × 15 cm) that extended from a common central platform (5×5 cm). During a 5 min observation period the following parameters were measured: (1) percentage of time spent in open arms, an inverse measure of anxiety-like behavior, calculated as (time in open arms/total time in arms) × 100; (2) percentage of entries in open arms, calculated as (number of entries with both mouse forepaws in open arms/total entries in arms) × 100; (3) stretched attend posture, measured as number of exploratory postures in which the body is stretched forward then retracted to the original position without any forward locomotion; (4) head dipping, measured as number of exploratory movements of head and shoulders over the side of the maze.

Depression-Related Tests

The FST was performed as previously described (Bambico et al., 2010). Briefly, 30 min after either desipramine (20 mg/kg) or vehicle administration, mice were placed individually into Plexiglas cylindrical bins (20 cm diameter, 50 cm high) filled with water (25–27°C water temperature) to a depth of 20 cm. Desipramine was dissolved in saline and injected intraperitoneally in a volume of 10 ml/kg of body weight. The immobility time was the ethologically relevant parameter, and each mouse was considered immobile when making only those movements necessary to keep its head above water. The mice were allowed to swim for 6 min and the total duration of activity was determined during the last 4 min.

The TST was performed as previously described (Bambico et al., 2010). In particular, the mouse was suspended by the tail from a lever in a $30 \times 30 \times 30$ cm white-painted enclosure, 30 min after either desipramine (20 mg/kg) or vehicle administration (intraperitoneally). Movements were recorded and quantified for 6 min, although only the last 5 min were used for analysis. Immobility was defined as hanging passively and completely motionless.

For our SPT, mice were isolated in small cages ($22.5 \times 16.7 \times 14$ cm). They each had free access to two drinking bottles, one filled with 250 ml tap water and the other with a 2% sucrose solution. Prior to testing, there was a 48h adaptation period to habituate to the different types of fluid. The mice were subsequently deprived from food and liquids for 3h. During the next 24h, free consumption of water and 2% sucrose solution took place, in the presence of *ad libitum* food. Fluid intake was measured afterwards by weighing the drinking bottles. Sucrose preference was calculated from the amount of sucrose solution consumed, expressed as a percentage of the total amount of liquid drunk.

Microdialysis in Freely-Moving Mice and HPLC Analysis

The microdialysis was performed according to Cassano et al. (2012). Briefly, anaesthetized mice were double-implanted with both a CMA/7 probe (6 kDa cut-off; 2 mm membrane length; CMA Microdialysis) placed vertically into the right vHIPP (anterior-posterior, -3.0 mm; lateral, +3.0 mm; ventral, -1.8 mm from bregma; Figure 2B) and a hand-made microdialysis linear probe (AN69 Hospal S.p.A; 20 kDa cut-off; 3 mm membrane length) placed horizontally into the FC (anterior-posterior, +5.9 mm; ventral, -4.0 mm from interaural line; Figure 2A) according to the stereotaxis atlas of Franklin and Paxinos (1997).

The day of the experiment, each probe was perfused with a Krebs-Ringer phosphate (KRP) buffer at a flow rate of 1 μl/min and dialysates were collected every 30 min. The constituents of the KRP buffer were (in mM) NaCl 145, KCl 2.7, $MgCl_2$ 1, $CaCl_2$ 2.4, and Na_2HPO_4 2, buffered at pH 7.4.

Four samples were collected to establish stable baseline levels of dopamine (DA), noradrenaline (NA), serotonin (5-HT), and their respective metabolites: homovanillic acid, 3-methoxy-4-hydroxyphenylethyleneglycol, and 5-hydroxyindoleacetic acid.

Thereafter, in order to investigate the effects of potassium (K^+) stimulation on cortical and hippocampal aminergic neurotransmitters, both probes were perfused for 30 min with KCl (100 mM)-enriched KRP buffer and then a further 6 samples were collected with the previous KRP buffer. Finally, probe placements were verified histologically.

The levels of aminergic neurotransmitters and their metabolites were determined by high liquid performance chromatography (HPLC), as previously described by Cassano et al. (2011).

Immunohistochemistry

Immunohistochemical staining for Aβ and tau were performed as previously described (Oddo et al., 2003b; Cassano et al., 2011, 2012; Bedse et al., 2014).

Briefly, 50 μm thick free-floating coronal sections were incubated with the following antibodies: mouse monoclonal 6E10 antibody (1:3000 dilution, Signet Laboratories) for total amyloid; and human-specific anti-tau antibody HT7 (1:1000 dilution, Pierce Biotechnology). Sections were developed with a diaminobenzidine substrate using the avidin-biotin horseradish peroxidase system (1:200 dilution, Vector Laboratories).

For TH and TPH immunostaining, sections were treated with 0.3% H_2O_2 in methanol for 20 min to inactivate endogenous peroxidase, were exposed to blocking serum (2% normal goat serum) for 1h at room temperature, and were incubated overnight at room temperature with an anti-mouse biotinylated antibody (1:600 dilution Anti-TH, Millipore; 1:1000 dilution Anti-TPH, Sigma). Sections were washed and then incubated in biotinylated goat antimouse serum (1:500 dilution, Jackson ImmunoResearch) for 60 min at room temperature. After an additional 10 min rinsing with 0.1M PB, sections were treated with the avidin-biotin horseradish peroxidase system and developed with diaminobenzidine.

All stained sections were dehydrated in ascending ethanol concentrations, cleared in xylene, and mounted with the Eukitt mounting medium (Sigma-Aldrich). Slice images were captured using a Nikon 80i Eclipse microscope (Nikon, Tokyo, Japan) and the intensity of each protein's immunostaining was measured semi-quantitatively as regional optical density using the Scion Image software. The averaged optical densities of non-immunoreactive regions of each section were used for background normalization.

Statistical Analyses

All data were expressed as mean ± SEM. Most of the behavioral data failed to meet the homoscedasticity assumption. In fact, within-group variability was analysed through Levene test for homogeneity of variances; therefore, data were analyzed by Mann-Whitney non-parametric U test (data from the OFT, EPMT, and SPT) and Kruskal–Wallis ANOVA followed by orthogonal chi-square (χ^2) partitioning to test the main effects of genotype, treatment, and genotype-by-treatment interaction, each with one degree of freedom (χ^2_1). A Mann–Whitney U test with Bonferroni's correction was used as the post hoc test for multiple comparisons.

Neurochemical data were homoscedastic, as shown by the Levene test for homogeneity of variances; therefore, data were analyzed by two-way ANOVA for repeated measures, with time as the within variable and genotype as the between variable. Dunnett's and Bonferroni's post hoc comparisons were used where appropriate. Unpaired *t*-tests were used to evaluate differences between genotypes for the average basal extracellular levels of each of the neurotransmitters and their metabolites (obtained as the marginal means of the 4 baseline samples).

Immunohistochemical results were calculated as a percentage of controls. The intensity of Aβ, tau, TH, and TPH immunostaining was measured semi-quantitatively as regional optical density. For each animal, measurements were obtained in at least 3 consecutive sections containing the region of

interest. For each region of interest, the results were analyzed by unpaired t-test. Because of the difference in the number of slides examined, the error degrees of freedom were kept constant at 6 based on the number of animals per group (n = 4). The threshold for statistical significance was p < 0.05.

Results

Anxiety-Like Phenotype in 3×Tg-AD Mice

Statistical analysis of the ethological parameters measured in the OFT revealed that both rearing frequency and rearing duration were significantly lower in 3×Tg-AD than in non-Tg mice (frequency: -68%, U = 1.5, n = 8 per group, p = 0.0016; duration: -60%, U = 7.0, n = 8 per group, p = 0.0099; Figure 1A and B, respectively). As for thigmotaxis, although not significant, 3×Tg-AD mice spent more time in the corners and along the walls compared to non-Tg mice (+21%, U = 18.5, n = 8 per group, p = 0.1719; Figure 1C); likewise, statistical analysis of grooming behavior showed a trend toward an increase in 3×Tg-AD mice compared to non-Tg mice (+133%, U = 27, n = 8 per group, p = 0.6454; Figure 1D).

Statistical analysis of the ethological parameters measured in the EPMT did not reveal any overall difference between mutant and non-Tg mice (Figure 1E–H). In particular, no differences between genotypes were observed in the percentage of time spent in open arm (U = 21, n = 8 per group, p = 0.2691), the percentage of entries in open arm (U = 31.5, n = 8 per group, p = 1.0), stretched attend posture (U = 19.0, n = 8 per group, p = 0.1352), or head dipping (U = 16.50, n = 8 per group, p = 0.1117).

As we have already reported, mouse locomotor activity measured as number of squares crossed during the 30 min session was identical in both genotypes (Cassano et al., 2011).

Depressive-Like Phenotype in 3×Tg-AD Mice

We next tested the depressive-like phenotype of 3×Tg-AD mice in two models of stress-coping behavior (FST and TST) and with an anhedonia test.

Figure 1I presents the behavioral profile in the FST comparing differences in immobility. Kruskal-Wallis ANOVA for immobility time revealed the following significant differences: H = 31.64, df = 3, p < 0.001, n = 10 per group. The orthogonal partitioning of the Kruskal-Wallis H revealed a significant main effect of genotype (X^2_1 = 18.61, p = 0.0001) and treatment (X^2_1 = 12.94, p = 0.0003), but not genotype-by-treatment interaction (X^2_1 = 0.041, p = 0.84). Post hoc comparisons showed that the immobility duration was higher (p < 0.05) in vehicle-treated 3×Tg-AD mice than in vehicle-treated non-Tg mice. Moreover, the administration of desipramine significantly reduced (p < 0.05) the immobility duration only in non-Tg mice but not in 3×Tg-AD mice, therefore a significant difference (p < 0.05) between them was still observed after drug treatment.

Figure 1J presents the behavioral profile of 3×Tg-AD and non-Tg mice in the TST. Kruskal-Wallis ANOVA for immobility time showed the following significant differences: H = 28.43, df = 3, p < 0.001, n = 10 per group. The orthogonal partitioning of the Kruskal-Wallis H revealed a significant main effect of genotype (X^2_1 = 19.56, p = 0.0001) and treatment (X^2_1 = 8.14, p = 0.004), but not genotype-by-treatment interaction (X^2_1 = 0.703, p = 0.402). Post hoc comparisons showed that the immobility duration was higher (p < 0.05) in vehicle-treated 3×Tg-AD mice than in vehicle-treated non-Tg mice. The administration of desipramine significantly decreased (p < 0.05) the immobility duration

in non-Tg mice but not in the 3×Tg-AD mice, therefore a significant difference (p < 0.05) between them was still observed after drug treatment.

Figure 1K presents the behavioral profile of 3×Tg-AD and non-Tg mice in the SPT. We found a significantly increased preference for sucrose in the non-Tg group compared to the 3×Tg-AD mice (U = 6.0, n = 9 per group, p = 0.0019). The effect was not accounted for by a difference in total fluid intake (fluid intake non-Tg mice: 10.22±1.579, n=9 per group; fluid intake 3×Tg-AD mice: 10.00±1.616, n=9 per group). The increased preference by non-Tg mice for sucrose is consistent with an antidepressant-like phenotype suggested by results in the FST and TST.

Impaired Basal Aminergic Neurotransmitter Function in 3×Tg-AD Mice

Since basal extracellular aminergic neurotransmitters in each brain region of non-Tg mice and 3×Tg-AD mice did not differ significantly across experiments, the basal values for each experimental group were pooled and taken as an average of dialysate samples 1–4, measured after a 2 hour stabilization period. NA, DA, 5-HT (see histograms in Figure 2C, E, and G), and their metabolite (see Table 1) levels were significantly reduced in the FC of 3×Tg-AD mice compared to the control group; likewise, the basal NA (see histogram in Figure 2D) and 3-methoxy-4-hydroxyphenylethyleneglycol (see Table 1) levels in vHIPP of 3×Tg-AD mice were respectively reduced by 35% and 46% compared with non-Tg mice. DA (see histogram in Figure 2F) and its major metabolite, homovanillic acid (see Table 1), were not different in the vHIPP of the two genotypes. Moreover, due to the experimental conditions of analysis, we were not able to detect the 5-HT levels in the vHIPP; nevertheless, the basal level of the 5-HT major metabolite, 5-hydroxyindoleacetic acid was significantly reduced by 62% in the vHIPP of 3×Tg-AD mice compared to non-Tg mice (see Table 1).

Impaired K+-Evoked Output of Aminergic Neurotransmitters in 3×Tg-AD Mice

As shown in Figure 2C and D, two-way ANOVA revealed that K+ stimulation significantly raised extracellular NA release in both genotypes, either in the FC [$F_{(time)7,91}$ = 6.815, p < 0.001; $F_{(time \times genotype)7,91}$ = 4.716, p < 0.001; $F_{(genotype)1,13}$ = 2.495, n.s.; 3×Tg-AD mice, n = 6; non-Tg mice: n = 9] and vHIPP [$F_{(time)7,119}$ = 6.231, p < 0.001; $F_{(time \times genotype)7,119}$ = 3.076, p < 0.05; $F_{(genotype)1,17}$ = 3.785, n.s.; 3×Tg-AD mice, n = 11; non-Tg mice, n = 8]. However, between-genotype comparisons (Tukey's test) indicated that K+-induced increases in NA levels were significantly attenuated in 3×Tg-AD mice in both brain regions. Cortical extracellular NA reached 331 and 111 pg/ml in non-Tg (186% of basal values) and 3×Tg-AD mice (168% of basal values), respectively, whilst hippocampal NA levels rose to 98 and 54 pg/ml in non-Tg (182% of basal values) and 3×Tg-AD mice (155% of basal values), respectively.

As far as the K+-evoked extracellular release of DA, we observed a surprising difference between genotype, and the disparity was confirmed in both brain regions (Figure 2E and F). In fact, the two-way ANOVA for repeated measures (actual values, mean of baseline and seven consecutive samples after high K+ retrodialysis administration) showed the following differences: in the FC, $F_{(time)7,91}$ = 7.610 with p < 0.001, $F_{(time \times genotype)7,91}$ = 7.447 with p<0.001, and $F_{(genotype)1,13}$ = 11.05 with p < 0.01 (3×Tg-AD mice, n = 8; non-Tg mice, n = 7); and in the vHIPP, $F_{(time)7,98}$ = 8.374 with p < 0.001, $F_{(time \times genotype)7,98}$ = 7.118 with p < 0.001, and $F_{(genotype)1,14}$ = 10.04 with p < 0.01 (3×Tg-AD mice, n = 9;
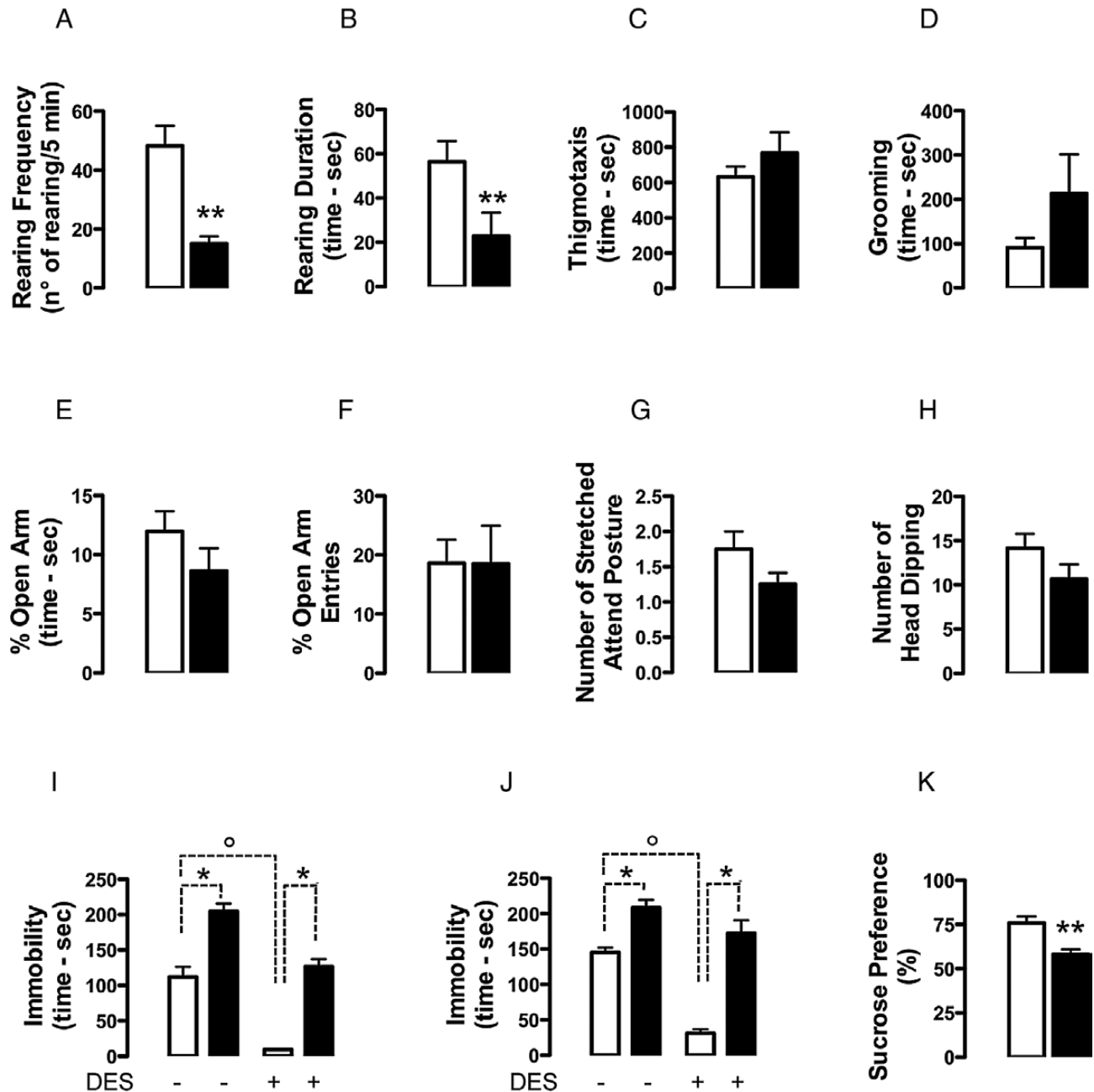
Figure 1. Evaluation of the emotional phenotype of 18-month-old 3×Tg-AD (black bars) and age-matched non-Tg mice (open bars). Aged 3×Tg-AD mice showed anhedonia features accompanied by depressive-like, but not anxiogenic-like phenotypes. Mice were tested in the OFT (A–D), EPMT (E–H), FST (I), TST (J), and SPT (K). 3×Tg-AD mice showed significantly lower rearing frequency (A) and rearing duration (B), whereas no differences were observed in the thigmotaxis (C) and grooming behavior (D) between genotypes. Genotype did not significantly influence the ethological parameters measured in the EPMT (E–H). Compared to the non-Tg counterpart, 3×Tg-AD mice spent significantly more time immobile in the FST (I) and TST (J); desipramine decreased the immobility duration only in the non-Tg mice, both in FST (I) and TST (J). The non-Tg group showed a significantly higher sucrose preference compared to the 3×Tg-AD mice (K). Data are expressed as mean ± S.E.M. *$p < 0.05$, **$p < 0.01$, main effect of genotype; °$p < 0.05$, main effect of desipramine-treatment.

non-Tg mice, n = 7). In particular, a high K⁺ challenge significantly increased extracellular DA release in both the FC and vHIPP of non-Tg mice (12141% and 5421% of basal value, respectively), but had no significant effect in the same brain regions of 3×Tg-AD mice (247% and 251% of basal value, respectively).

As well as dopaminergic transmission, depolarization-induced 5-HT release in FC was significantly decreased in the 3×Tg-AD mice when compared with non-Tg mice (Figure 2G). In this regard, the two-way ANOVA for repeated measures

(actual values, mean of baseline and seven consecutive samples after high K⁺ retrodialysis administration) showed the following results in the FC: $F_{(time)7,84} = 5.392$ with $p < 0.001$, $F_{(time \times genotype)7,84} = 2.813$ with $p < 0.05$, and $F_{(genotype)1,12} = 8.046$ with $p < 0.05$ (3×Tg-AD mice, n = 6; non-Tg mice, n = 8). In particular, in non-Tg mice 5-HT reached 2668 pg/ml (225% of basal values) after 30 min of high K⁺ retrodialysis administration, whereas at the same time-point extracellular 5-HT levels peaked at 537 pg/ml (177% of basal values) in 3×Tg-AD mice.
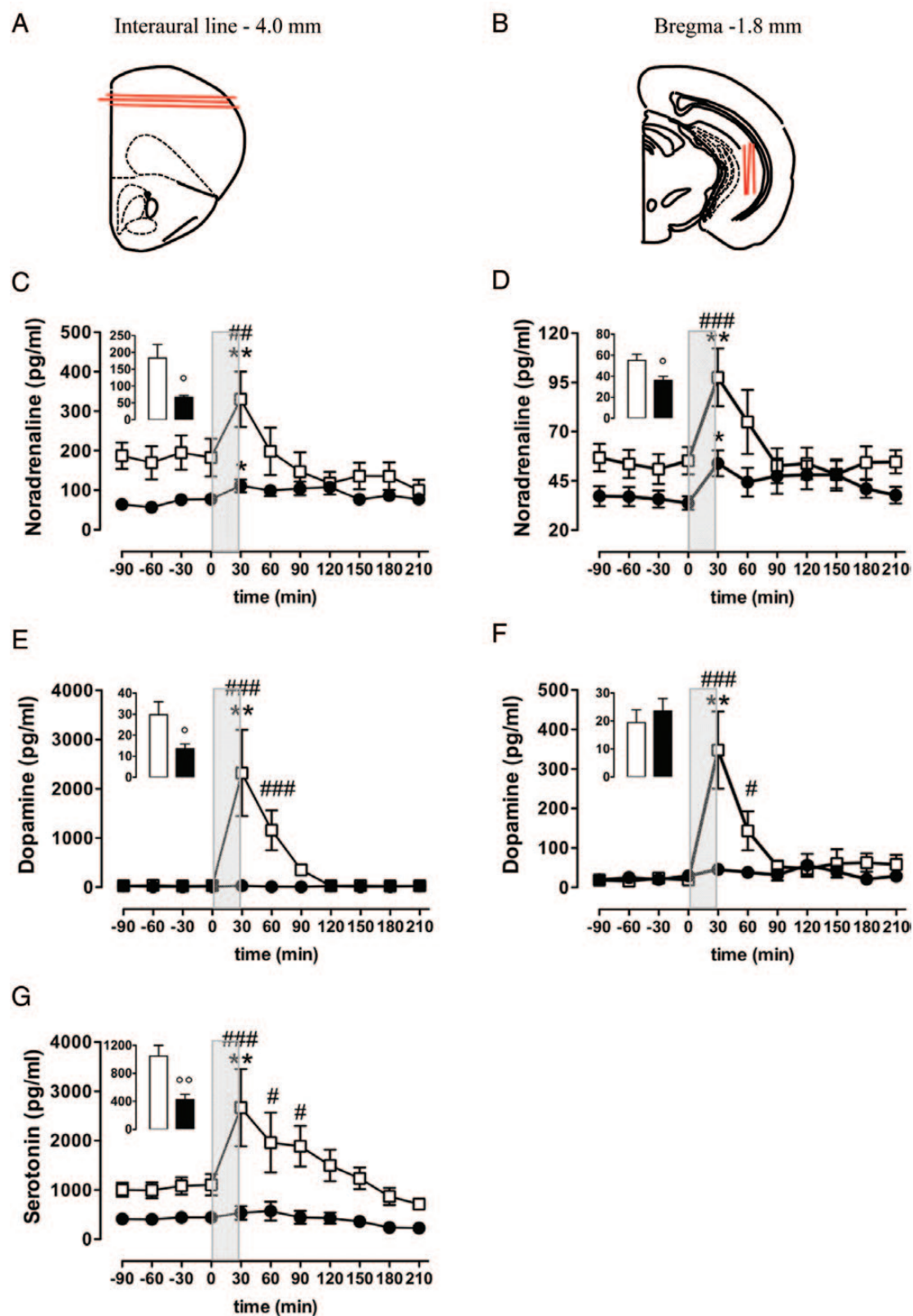
Figure 2. Basal and K+-evoked release of NA (C–D), DA (E–F), and 5-HT (G) in the FC (C, E, and G) and ventral hippocampus (D and F) of conscious, freely-moving non-Tg (open squares) and 3×Tg-AD (black circles) 18-month-old mice. (C–G) Inserts represent average baseline levels (marginal means from -90 to 0 minutes) observed in non-Tg (open bars) and 3×Tg-AD (black bars) mice; grey areas indicate the perfusion with KCl-enriched (100 mM) Krebs-Ringer phosphate (KRP) buffer. Data are expressed as mean ± S.E.M. °p < 0.05 and °°p < 0.01 versus non-Tg mice (unpaired student t-test). *p < 0.05 and **p < 0.01 versus last baseline within the same group (Dunnett's multiple comparison test). #p < 0.05, ##p <0.01, ###p < 0.001 versus 3×Tg-AD mice (Tukey test for between-groups comparisons). (A) and (B) Brain diagrams illustrating the average sites (red lines) where microdialysis probes were implanted and where the representative microphotographs were taken.

Table 1. Basal Extracellular Level of Monoamine Metabolites (ng/ml) in the FC and vHIPP of 18-Month-Old 3×Tg-AD and Non-Tg Mice.

	Frontal cortex				Ventral hippocampus			
	MOPEG	DOPAC	HVA	5-HIAA	MOPEG	DOPAC	HVA	5-HIAA
Non-Tg	9.0±1.0 (n=9)	47.0±12.1 (n=9)	68.2±10.4 (n=9)	67.7±11.7 (n=9)	1.9±0.4 (n=10)	0.7±0.2 (n=8)	1.0±0.1 (n=10)	22.0±2.9 (n=10)
3×Tg-AD	5.5±0.8* (n=7)	6.9±2.1** (n=9)	31.2±7.9* (n=9)	30.9±6.5* (n=8)	1.0±0.1* (n=9)	0.04±0.02* (n=8)	0.8±0.1 (n=9)	8.4±1.9* (n=8)

Data are expressed as mean ± S.E.M. *p < 0.05 and **p < 0.01 versus non-Tg mice (unpaired student's t-test)

3×Tg-AD mice Show Diffuse Pathologies Without Gross Alterations in Immunostaining

The 3×Tg-AD mice showed extracellular Aβ deposits and human tau-reactive neurons in the cortical and some subcortical regions (Figure 3). In particular, although Aβ deposits were observed in the FC, caudatus putamen, amygdala, and vHIPP, the ventral midbrain (substantia nigra, ventral tegmental area, and dorsal raphe) and brainstem regions (locus coeruleus) were generally free of Aβ deposits. Moreover, extensive human tau immunoreactivity in 3×Tg-AD mice was particularly evident in the FC, all the forebrain regions analyzed (caudatus putamen, nucleus accumbens, and amygdala), the vHIPP, and the locus coeruleus. None of these immunoreactive structures were detected in non-Tg brains.

To determine whether Aβ and tau pathologies were associated with abnormalities in monoaminergic systems, sections from brains of 18-month-old 3×Tg-AD and non-Tg mice were immunostained for TH and TPH (Figure 4). Despite the neuropathological hallmarks of AD being spread out in different brain regions of the mutant mice, surprisingly, we observed few significant differences between genotypes in the TH and THP immunostaining. In particular, TH+ neurons were significantly lower (-16%) in the caudatus putamen, as well as TPH+ neurons (-16%) in the dorsal raphe of 3×Tg-AD compared to non-Tg mice. Conversely, the vHIPP showed a significant increase of TPH+ neurons (+22%) in the mutant mice compared to control mice.

Discussion

The results of the present study demonstrate that depressive–like but not anxiogenic-like phenotypes co-exist with deficits of monoaminergic neurotransmissions in 18-month-old 3×Tg-AD mice, which show substantial amounts of amyloid plaques and tau pathologies in their cortical regions and limbic areas. Moreover, we observed that desipramine did not reverse the depressive-like phenotype in 3×Tg-AD mice. The current study provides a comprehensive evaluation of depression-like and anhedonia features in 3×Tg-AD mice. To our knowledge, only a few studies have evaluated the nonmnemonic characteristics of the 3×Tg-AD model (Giménez-LIort et al., 2007; Pietropaolo et al., 2008; España et al., 2010; Sterniczuk et al., 2010; Filali et al., 2012), but none of them have fully evaluated such specific noncognitive domain.

In our study we found that 3×Tg-AD mice exhibited higher immobility time compared with non-Tg mice in the FST and TST. In contrast, the motor function and anxiety-related emotional response of the 3×Tg-AD mice were normal, although we observed a significant reduction of the frequency and the duration of rearing events. None of the other parameters evaluated in the OFT and EPMT were able to differentiate between genotypes, as preoviously reported (Giménez-LIort et al., 2007; Pietropaolo et al., 2008; Pietropaolo et al., 2009). Furthermore, 3×Tg-AD mice showed body weights that were not significantly different from non-Tg mice. Therefore, the enhanced immobility time of 3×Tg-AD mice is unlikely to have been caused by a deficit in motor function, a change in their anxiety level, or an increase in body weight. Differently, an increased level of anxiety was found by other authors (Sterniczuk et al., 2010; Filali et al., 2012), when 3×Tg-AD mice were tested in the EPMT. In particular, Sterniczuk and colleagues (2010) tested younger 3×Tg-AD female mice (6 mice with mean age 9.25 months), whereas Filali and colleagues (2012) tested 12-month-old 3×Tg-AD female mice showing an increased anxiety, though only with the head-dipping measure.

Furthermore, España and colleagues (2010) found that 6-month-old 3×Tg-AD male mice showed a significant increase of freezing responses in the brightly-lit-chamber test compared to nontransgenic mice, when they were exposed to an anxiogenic stimulus such as a bright light (1850 lux).

Therefore, the discrepancy may be attributed to the differences in the experimental contexts (dim versus bright light), and mostly due to the use of different ages and sexes, which may have affected the assessment of the anxiety-like phenotype in our experiments versus those reported by other authors. In fact, it has been already shown that the female (but not male) 3×Tg-AD mice showed increased anxiety (Pietropaolo et al., 2009).

Moreover, 3×Tg-AD mice showed a significant decrease in sucrose preference, a putative indicator of anhedonia in rodents. Taken together, our results are consistent with the hypothesis of increased depression-like behavior and hedonic deficit in our murine model of AD; these data are concordant with findings of increased apathy and depression in Alzheimer patient (Ballard et al., 2008).

Hypothalamic-pituitary-adrenal axis alteration, which is known to be involved in the etiopathology of depression (Belmaker and Agam, 2008; Yu et al., 2008; Wuwongse et al., 2010), has been observed in 3×Tg-AD mice from 9 months of age (Green et al., 2006); therefore, we cannot rule out that the depressive-like behavior observed in aged 3×Tg-AD mice might be due to their higher plasma corticosterone levels and altered glucocorticoid receptor and corticotropin-releasing hormone compared to age-matched non-Tg mice (Green et al., 2006; Hebda-Bauer et al., 2013).

Interestingly, we observed that the NA reuptake inhibitor, desipramine, did not reduce the immobility time in the 3×Tg-AD mice. These results are in line with clinical evidences where conventional antidepressants have not been found to be effective in depression associated with AD (Pomara and Sidtis, 2007). In this regard, a recent systematic review evaluated the efficacy and safety of antidepressants compared with placebos in treating depression in patients with dementia (Leong, 2014). The author highlighted that the evidence for antidepressants in the treatment of depression in individuals with dementia is inconclusive (Leong, 2014). The American Psychiatric Association (2007) and the Canadian Medical Association Journal (2008) both recommended a trial of an antidepressant to treat clinically-significant, persistent depressed mood in demented patients. Serotonin reuptake inhibitors were the preferred agents based
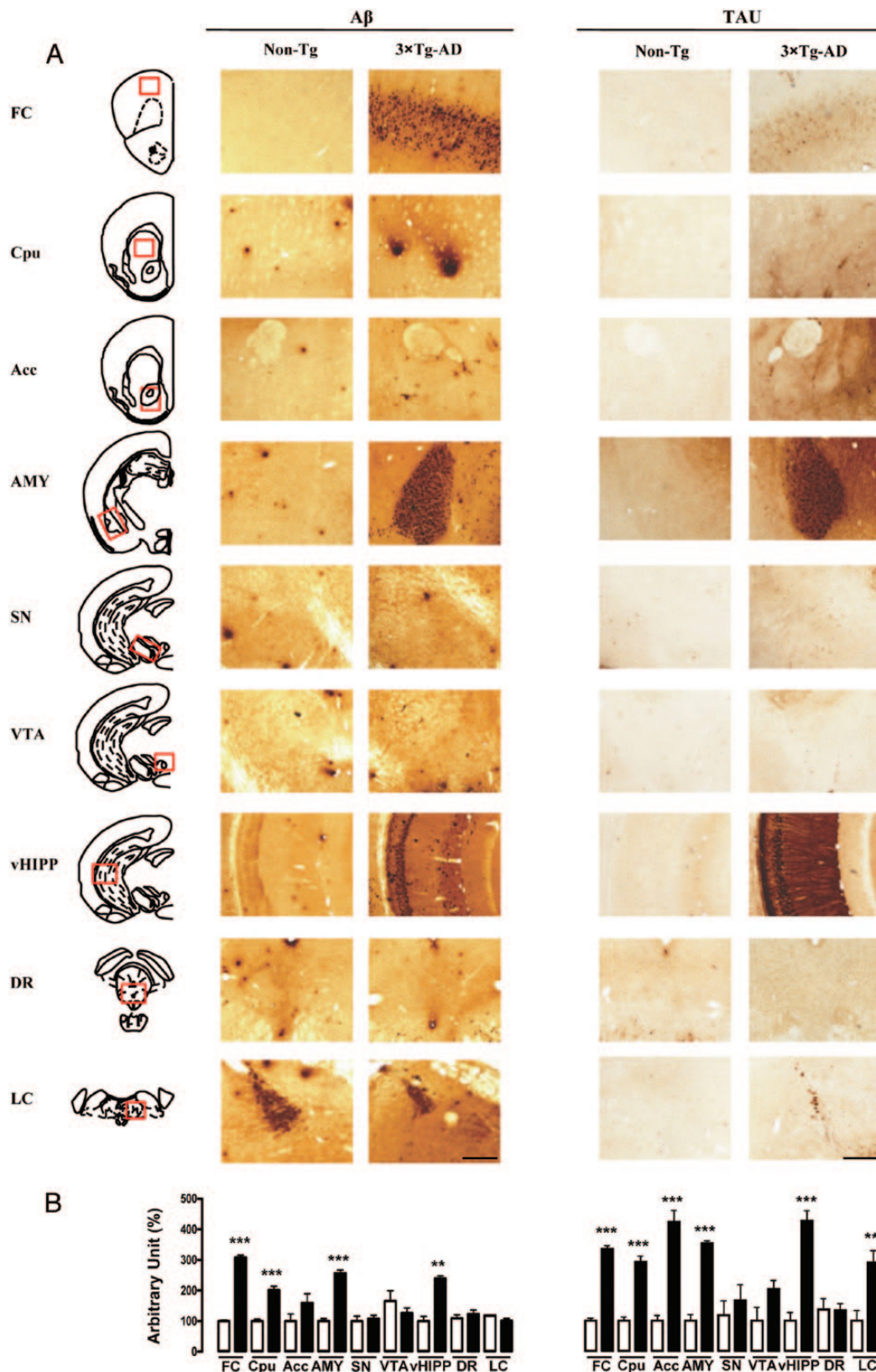
Figure 3. Representative microphotographs (2x magnification, scale bar 100 μm; A) and results obtained from the semi-quantitative analyses (B) of Aβ and tau immunostaining, taken from 50 μm-thick brain coronal sections obtained from non-Tg (white bars) and 3×Tg-AD (black bars) mice. The red squares within the brain diagrams illustrate the sites where the representative microphotographs were taken. The data are means ± SEM. **p < 0.01 and ***p < 0.001 versus non-Tg mice (unpaired student's t-test, n = 4 per group). FC: frontal cortex; Cpu: caudatus putamen; Acc: nucleus accumbens; AMY: amygdala; SN: substantia nigra; VTA: ventral tegmental area; vHIPP: ventral hippocampus; DR: dorsal raphe; LC: locus ceruleus.
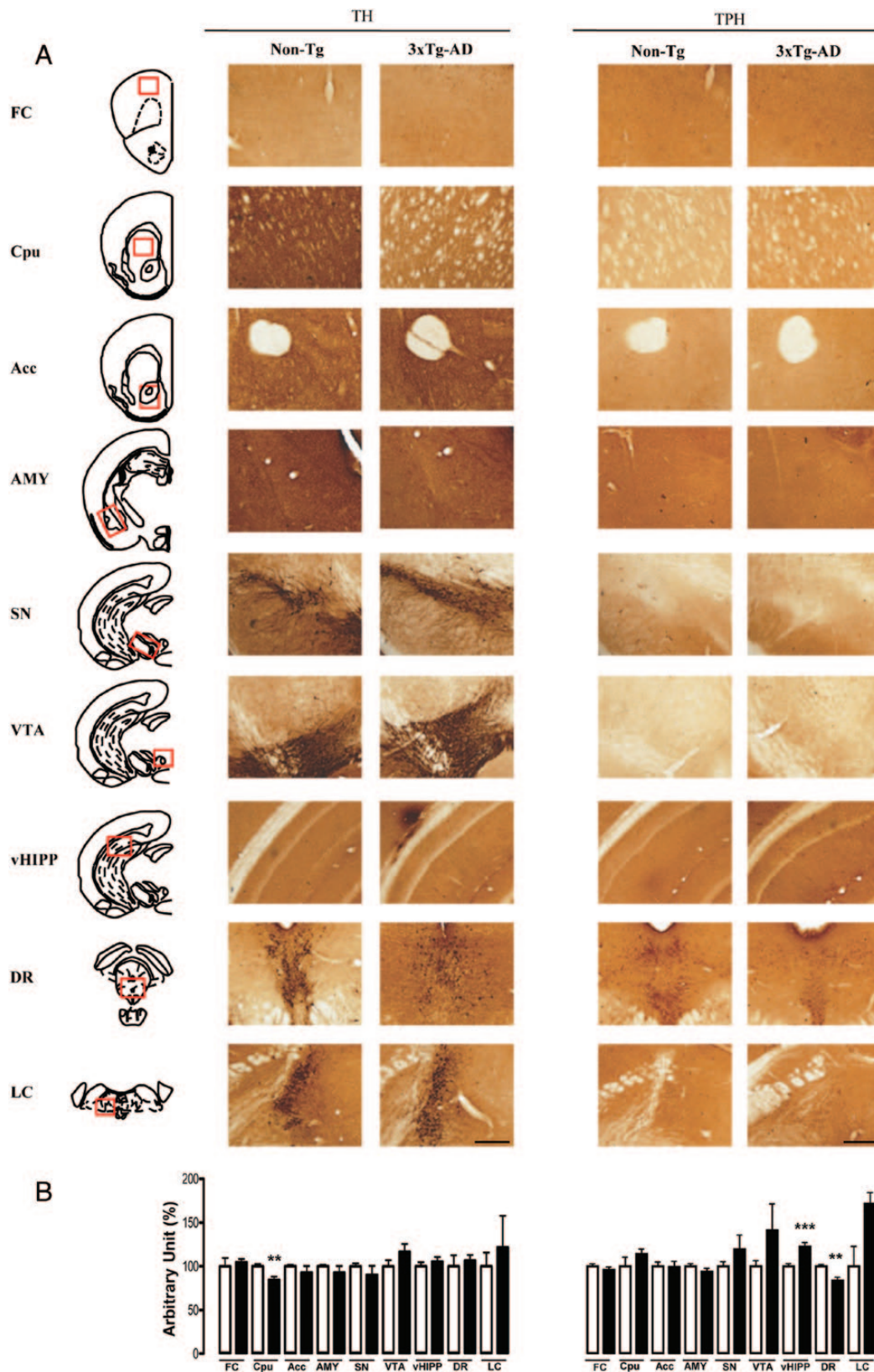
Figure 4. Representative microphotographs (2x magnification, scale bar 100 μm; A) and results obtained from the semi-quantitative analyses (B) of TH and TPH immunostaining, taken from 50 μm-thick brain coronal sections obtained from non-Tg (white bars) and 3 × Tg-AD (black bars) mice. The red squares within the brain diagrams illustrate the sites where the representative microphotographs were taken. The data are means ± SEM. **p < 0.01 and ***p < 0.001 versus non-Tg mice (unpaired student's t-test, n = 4 per group). FC: frontal cortex; Cpu: caudatus putamen; Acc: nucleus accumbens; AMY: amygdala; SN: substantia nigra; VTA: ventral tegmental area; vHIPP: ventral hippocampus; DR: dorsal raphe; LC: locus ceruleus.

on their tolerability profile (minimal anticholinergic activity) compared with other classes of antidepressants. However, a systematic review did not support the efficacy of serotonin reuptake inhibitor treatment for symptoms of comorbid depression in AD (Sepehry et al., 2012). In contrast, all three major antidepressant classes (tricyclics, selective serotonin re-uptake inhibitors, and monoamine oxidase inhibitors) appear effective in the treatment of depression in the non-demented elderly compared to placebo (Wilson et al., 2008). Therefore, in accordance with other authors, we agree that depression in dementia is likely different from depression in aging, and that its treatment cannot be extrapolated from treatment approaches in the normal elderly. Hence, such evidences prompted us to explore whether a depressive-like phenotype correlates with alterations of monoamine neurotransmitters in the AD model. In particular, with the exception of the hippocampal dopaminergic system, we found a significant reduction in basal extracellular release of the monoamine neurotransmitters in both the FC and vHIPP of 18-month-old 3×Tg-AD mice versus non-Tg mice. Although not significant, the basal output of the DA and its metabolite, homovanillic acid, in the vHIPP was reduced (-21% and -13%, respectively) in the 3×Tg-AD mice.

Likewise, Guzmàn-Ramos et al. (2012) showed that the basal levels of NA were lower than those of controls in both the insular cortex and the dorsal hippocampus of 10-month-old 3×Tg-AD mice; moreover, they found that the basal DA levels were significantly lower in the 3×Tg-AD mice compared to non-Tg mice only in the insular cortex. It has been demonstrated that synaptophysin, a presynaptic vesicle marker commonly used as an estimate of synaptic density, is not altered in either the cortex or the hippocampus of either genotype (Chen et al., 2000; Oddo, Caccamo, Kitazawa, et al. 2003; Oddo et al., 2003b; Cassano et al., 2012); therefore, it is unlikely that the lower basal levels of amines might be due to a synaptic loss.

Moreover, the pattern of monoamine release in response to K⁺ stimulation resulted in complete disruption in both the FC and vHIPP of 3×Tg-AD mice, but not in non-Tg mice. In particular, 30 min from the beginning of K⁺ stimulation, we observed a blunted NA release above the baseline in the FC (+60% in 3×Tg-AD versus +80% in non-Tg) and vHIPP (+50% in 3×Tg-AD versus +80% in non-Tg). Conversely, we observed a complete absence of DA peak release in response to K⁺ stimulation in both brain regions; likewise, 5-HT did not respond to a K⁺ depolarizing stimulus in the FC.

We have recently demonstrated that the complete absence of neurotransmitter peak release in response to K⁺ stimulation is consistent with a low energy level in the brain region, which, in turn, might be insufficient to ensure all those neuronal functions stimulated by K⁺, such as axonal transport, exocytosis, and the activity of the Na⁺/K⁺ ATPase pump (Cassano et al., 2012). Likewise, we cannot rule out that alterations of the molecular mechanisms governing synaptic vesicle trafficking and neurotransmitter release might account for the altered response to K⁺ stimulation. In fact, we have demonstrated that the 25-kDa synaptosomal-associated protein (SNAP-25), one of the synaptic vesicle exocytosis proteins in the soluble N-ethylmaleimide-sensitive factor attachment protein receptors, was significantly reduced in the hippocampus of 3×Tg-AD mice compared with non-Tg mice, whereas no difference was observed in the FC (Cassano et al., 2012).

Extracellular aminergic levels are tightly coupled to the activity of brain TH and TPH, two rate-limiting enzymes in the synthesis of DA, NA, and 5-HT. Given the decreases in the aminergic system in the FC and vHIPP of 3×Tg-AD mice,

we quantified the level of both enzymes in different brain regions. Besides a significant reduction in the caudatus putamen of 3×Tg-AD mice, no effect of genotype on the levels of TH was observed, suggesting that the differences in amine and metabolite levels cannot be explained by a decrease of TH levels (or by a decrease in the number of TH-positive neurones). Our result agrees with one clinical study, where authors have demonstrated decreased levels of striatal TH in post-mortem brain tissue taken from patients with AD when compared to control brains (Nagatsu and Iizuka, 1989). Just as with the TH, surprisingly, we found modest alterations of TPH expression among the brain regions, which cannot account for the total lack of responsiveness to KCl stimulation in the FC. In particular, we found a significant increase of TPH expression in the vHIPP and a significant decrease in the dorsal raphe. Despite the effects described above, no differences in other brain regions were detected. Increased hippocampal 5-HT fiber density in the 18-month-old 3×Tg-AD were observed in proximity to amyloid plaques, suggesting that aberrant 5-HT neuronal sprouting and amyloid deposition are closely linked in AD neuropathology (Noristani et al., 2010). The massive build-up of plaques at a later age (18 months) may induce neurotoxic effects, resulting in neuronal damage that, in turn, may also stimulate an increase in 5-HT fibers in the hippocampus of 3×Tg-AD mice. Increased 5-HT fiber sprouting was also found after acute brain damage, such as Aβ, ibotenic acid, and NMDA injection in rats (Zhou et al., 1995; Harkany et al., 2000). Thus, serotonergic fiber sprouting may act as a compensatory mechanism to counteract Aβ- and tau-induced neurotoxicity. In fact, it has been reported that 5-HT fiber sprouting was further increased in the hippocampi of 24-month-old 3×Tg-AD mice, which showed massive extracellular Aβ plaques and large tau pathology (Noristani et al., 2011). Speculatively, it is conceivable that amyloid plaques and tau pathologies might profoundly disrupt the functioning of neurons that contain aminergic neurotransmitters in the pre-synaptic terminals, potentially leading to a depressive-like phenotype and, more interestingly, to a lack of response of antidepressant treatment.

Acknowledgments

Statement of Interest

None.

References

American Psychiatric Association (2007). Practice guideline for the treatment of patients with Alzheimer's disease and other dementias, second ed. Ann Intern Med 148:370–378.

Assal F, Cummings JL (2002) Neuropsychiatric symptoms in the dementias. Curr Opin Neurol 15:445–450.

Arsenault D, Julien C, Tremblay C, Calon F (2011) DHA improves cognition and prevents dysfunction of entorhinal cortex neurons in 3xTg-AD mice. PLOS ONE 6:e17397.

Ballard C, Lana MM, Theodoulou M, Douglas S, McShane R, Jacoby R, Kossakowski K, Yu LM, Juszczak E (2008) Investigators DART AD. A randomised, blinded, placebo-controlled trial in dementia patients continuing or stopping neuroleptics (the DART-AD trial). PLOS Med 5:e76.

Bambico FR, Cassano T, Dominguez-Lopez S, Katz N, Walker CD, Piomelli D, Gobbi G (2010) Genetic deletion of fatty acid amide hydrolase alters emotional behavior and serotonergic transmission in the dorsal raphe, prefrontal cortex, and hippocampus. Neuropsychopharmacology 35:2083–2100.

Bedse G, Romano A, Cianci S, Lavecchia AM, Elphick MR, LaFerla FM, Vendemiale G, Grillo C, Altieri F, Cassano T, Gaetani S (2014) Altered expression of the CB1 cannabinoid receptor in the triple transgenic mouse model of Alzheimer's disease. J Alzheimers Dis 40:701–712.

Belmaker RH, Agam G (2008) Major depressive disorder. N Engl J Med 358:55–68.

Billings LM, Oddo S, Green KN, McGaugh JL, LaFerla FM (2005) Intraneuronal Abeta causes the onset of early Alzheimer's disease-related cognitive deficits in transgenic mice. Neuron 45:675–688.

Carroll JC, Rosario ER, Chang L, Stanczyk FZ, Oddo S, LaFerla FM, Pike CJ (2007) Progesterone and estrogen regulate Alzheimer-like neuropathology in female 3xTg-AD mice. J Neurosci 27:13357–13365.

Cassano T, Romano A, Macheda T, Colangeli R, Cimmino CS, Petrella A, LaFerla FM, Cuomo V, Gaetani S (2011) Olfactory memory is impaired in a triple transgenic model of Alzheimer disease. Behav Brain Res 224:408–412.

Cassano T, Serviddio G, Gaetani S, Romano A, Dipasquale P, Cianci S, Bellanti F, Laconca L, Romano AD, Padalino I, LaFerla FM, Nicoletti F, Cuomo V, Vendemiale G (2012) Glutamatergic alterations and mitochondrial impairment in a murine model of Alzheimer disease. Neurobiol Aging 33:1121.e1–1121.e12.

Chen CP, Eastwood SL, Hope T, McDonald B, Francis PT, Esiri MM (2000) Immunocytochemical study of the dorsal and median raphe nuclei in patients with Alzheimer's disease prospectively assessed for behavioural changes. Neuropath Appl Neuro 26:347–355.

España J, Giménez-Llort L, Valero J, Miñano A, Rábano A, Rodriguez-Alvarez J, LaFerla FM, Saura CA (2010) Intraneuronal beta-amyloid accumulation in the amygdale enhances fear and anxiety in Alzheimer's disease transgenic mice. Biol Psychiatry 67:513–521.

Filali M, Lalonde R, Theriault P, Julien C, Calon F, Planel E (2012) Cognitive and non-cognitive behaviors in the triple transgenic mouse model of Alzheimer's disease expressing mutated APP, PS1, and Mapt (3xTg-AD). Behav Brain Res 234:334–342.

Franklin KBJ, Paxinos G (1997) The mouse brain in stereotaxic coordinates. San Diego, CA: Academic Press.

Giménez-Llort L, Blázquez G, Cañete T, Johansson B, Oddo S, Tobeña A, LaFerla FM, Fernández-Teruel A (2007) Modeling behavioral and neuronal symptoms of Alzheimer's disease in mice: a role for intraneuronal amyloid. Neurosci Biobehav Rev 31:125–147.

Gottfries CG (1990) Neurochemical aspects on aging and diseases with cognitive impairment. J Neurosci Res 27:541–547.

Green KN, Billings LM, Roozendaal B, McGaugh JL, LaFerla FM (2006) Glucocorticoids increase amyloid-beta and tau pathology in a mouse model of Alzheimer's disease. J Neurosci 26:9047–9056.

Guzmàn-Ramos K, Moreno-Castilla P, Castro-Cruz M, McGaugh JL, Martìnez-Coria H, LaFerla FM, Bermùdez-Rattoni F (2012) Restoration of dopamine release deficits during object recognition memory acquisition attenuates cognitive impairment in a triple transgenic mice model of Alzheimer's disease. Learn Mem 19:453–460.

Harkany T, Dijkstra IM, Oosterink BJ, Horvath KM, Abrahám I, Keijser J, Van der Zee EA, Luiten PG (2000) Increased amyloid precursor protein expression and serotonergic sprouting following excitotoxic lesion of the rat magnocellular nucleus basalis: neuroprotection by Ca2+ antagonist nimodipine. Neuroscience 101:101–114.

Hebda-Bauer EK, Simmons TA, Sugg A, Ural E, Stewart JA, Beals JL, Wei Q, Watson SJ, Akil H (2013) 3xTg-AD mice exhibit an activated central stress axis during early-stage pathology. J Alzheimers Dis 33:407–422.

Leong C (2014) Antidepressants for depression in patients with dementia: a review of the literature. Consult Pharm 29:254–263.

Modrego PJ, Ferrández J (2004) Depression in patients with mild cognitive impairment increases the risk of developing dementia of Alzheimer type: a prospective cohort study. Arch Neurol 61:1290–1293.

Nagatsu T, Iizuka R (1989) Tyrosine hydroxylase, tryptophan hydroxylase, and the biopterin cofactor in the brains from patients with Alzheimer's disease. J Neural Transm Park Dis Dement Sect 1:21.

Nelson RL, Guo Z, Halagappa VM, Pearson M, Gray AJ, Matsuoka Y, Brown M, Martin B, Iyun T, Maudsley S, Clark RF, Mattson MP (2007) Prophylactic treatment with paroxetine ameliorates behavioral deficits and retards the development of amyloid and tau pathologies in 3xTgAD mice. Exp Neurol 205:166–176.

Noristani HN, Olabarria M, Verkhratsky A, Rodríguez JJ (2010) Serotonin fibre sprouting and increase in serotonin transporter immunoreactivity in the CA1 area of hippocampus in a triple transgenic mouse model of Alzheimer's disease. Eur J Neurosci 32:71–79.

Noristani HN, Meadows RS, Olabarria M, Verkhratsky A, Rodríguez JJ (2011) Increased hippocampal CA1 density of serotonergic terminals in a triple transgenic mouse model of Alzheimer's disease: an ultrastructural study. Cell Death Dis 2:e210.

Nyberg P, Adolfsson R, Hardy JA, Nordberg A, Wester P, Winblad B (1985) Catecholamine topochemistry in human basal ganglia. Comparison between normal and Alzheimer brains. Brain Res 333:139–142.

Oddo S, Caccamo A, Kitazawa M, Tseng BP, LaFerla FM (2003a) Amyloid deposition precedes tangle formation in a triple transgenic model of Alzheimer's disease. Neurobiol Aging 24:1063–1070.

Oddo S, Caccamo A, Shepherd JD, Murphy MP, Golde TE, Kayed R, Metherate R, Mattson MP, Akbari Y, LaFerla FM (2003b) Triple-transgenic model of Alzheimer's disease with plaques and tangles: intracellular Abeta and synaptic dysfunction. Neuron 39:409–421.

Ojha J, Karmegam RV, Masilamoni JG, Terry AV, Cashikar AG (2011) Behavioral defects in chaperone-deficient Alzheimer's disease model mice. PLOS ONE 6:e16550.

Palmer AM, DeKosky ST (1993) Monoamine neurons in aging and Alzheimer's disease. J Neural Transm Gen Sect 91:135–159.

Pietropaolo S, Feldon J, Yee BK (2008) Age-dependent phenotypic characteristics of a triple transgenic mouse model of Alzheimer disease. Behav Neurosci 122:733–747.

Pietropaolo S, Sun Y, Li R, Brana C, Feldon J, Yee BK (2009) Limited impact of social isolation on Alzheimer-like symptoms in a triple transgenic mouse model. Behav Neurosci 123:181–195.

Pomara N, Sidtis J (2007) Possible therapeutic implication of Abeta disturbances in depression. Int J Geriatr Psychiatry 22:931–932.

Sepehry AA, Lee PE, Hsiung GY, Beattie BL, Jacova C (2012) Effect of selective serotonin reuptake inhibitors in Alzheimer's disease with comorbid depression: a meta-analysis of depression and cognitive outcomes. Drug Aging 29:793–806.

Steffens DC, Plassman BL, Helms MJ, Welsh-Bohmer KA, Saunders AM, Breitner JC (1997) A twin study of late-onset depression and apolipoprotein E epsilon 4 as risk factors for Alzheimer's disease. Biol Psychiatry 41:851–6.

Sterniczuk R, Antle MC, Laferla FM, Dyck RH (2010) Characterization of the 3xTg-AD mouse model of Alzheimer's disease: part 2. Behavioral and cognitive changes. Brain Res 1348:149–55.

Yao J, Irwin RW, Zhao L, Nilsen J, Hamilton RT, Brinton RD (2009) Mitochondrial bioenergetic deficit precedes Alzheimer's pathology in female mouse model of Alzheimer's disease. Proc Natl Acad Sci USA 106:14670–5.

Yu S, Holsboer F, Almeida OF (2008) Neuronal actions of glucocorticoids: focus on depression. J Steroid Biochem Mol Biol 108:300–309.

Wilson KC, Mottram PG, Vassilas CA (2008) Psychotherapeutic treatments for older depressed people. Cochrane Database Syst Rev 23:CD004853.

Wuwongse S, Chang RC, Law AC (2010) The putative neurodegenerative links between depression and Alzheimer's disease. Prog Neurobiol 91:362–375.

Zhou FC, Azmitia EC, Bledsoe S (1995) Rapid serotonergic fiber sprouting in response to ibotenic acid lesion in the striatum and hippocampus. Brain Res Dev Brain Res 84:89–98.